

Catalysis Science & Technology

Accepted Manuscript

This article can be cited before page numbers have been issued, to do this please use: S. Chansai, Y. Kato, W. Ninomiya and C. Hardacre, *Catal. Sci. Technol.*, 2024, DOI: 10.1039/D4CY00552J.



This is an Accepted Manuscript, which has been through the Royal Society of Chemistry peer review process and has been accepted for publication.

Accepted Manuscripts are published online shortly after acceptance, before technical editing, formatting and proof reading. Using this free service, authors can make their results available to the community, in citable form, before we publish the edited article. We will replace this Accepted Manuscript with the edited and formatted Advance Article as soon as it is available.

You can find more information about Accepted Manuscripts in the [Information for Authors](#).

Please note that technical editing may introduce minor changes to the text and/or graphics, which may alter content. The journal's standard [Terms & Conditions](#) and the [Ethical guidelines](#) still apply. In no event shall the Royal Society of Chemistry be held responsible for any errors or omissions in this Accepted Manuscript or any consequences arising from the use of any information it contains.

An *in-situ* DRIFTS-MS study on elucidating the role of V in the selective oxidation of methacrolein to methacrylic acid over heteropolyacid compounds

View Article Online
DOI: 10.1039/C4CY00552J

Sarayute Chansai^{a,*}, *Yuki Kato*^b, *Wataru Ninomiya*^b, and *Christopher Hardacre*^{a,*}

^a Department of Chemical Engineering, Engineering Building A, The University of Manchester, Manchester M13 9PL, U.K.

^b MMA Group, Monomers & Catalysts Laboratory, Mitsubishi Chemical Corporation, 20-1 Miyuki-cho, Otake-shi, Hiroshima 739-0693, Japan.

*Corresponding author: sarayute.chansai@manchester.ac.uk, c.hardacre@manchester.ac.uk

Abstract:

The role of vanadium in 11-molybdo-1-vanadophosphoric acid ($\text{H}_4\text{PMo}_{11}\text{VO}_{40}$, HPMoV) has been investigated and compared with 12-molybdophosphoric acid ($\text{H}_3\text{PMo}_{12}\text{O}_{40}$, HPMo) using *in-situ* diffuse reflectance infrared Fourier transform spectroscopy (DRIFTS) coupled with mass spectrometry (MS). It has been found for the first time that there are differences in the DRIFT spectra of carbonyl and carboxylate-type species recorded in the region of 1900 – 1200 cm^{-1} between the two compounds under methacrolein (MAL), MAL+O₂, and MAL+O₂+H₂O reaction conditions at 320 °C and the MS results show the faster formation of methacrylic acid over HPMoV than HPMo catalysts. A number of hydrocarbon species adsorbed on the surface have been identified in the DRIFTS including 5-membered ring of lactone-type adsorbed species, 6-membered ring of lactone-type adsorbed species, bidentate methacrylate adsorbed species, monodentate methacrylate adsorbed species, and π -adsorbed species with the presence of V in the heteropolyacid Keggin structure favouring the formation of monodentate methacrylate surface species compared with lactone-type surface species under MAL+O₂+H₂O reaction conditions at 320 °C. The monodentate methacrylate surface species



is proposed to be the intermediate in the final step for the formation of MAA. It is likely that the same mechanism of selective oxidation of MAL occurs with and without the substitution of Mo with V, with the presence of V resulting in a faster formation of active monodentate methacrylate intermediates.

Keywords:

Methacrolein, Methacrylic acid, *in-situ* DRIFTS-MS, Selective oxidation, Keggin unit, Heteropolyacids, $\text{H}_3\text{PMo}_{12}\text{O}_{40}$, $\text{H}_4\text{PMo}_{11}\text{VO}_{40}$

1. Introduction

Heteropolyacids (HPAs) used as oxidation catalysts have been extensively investigated for many decades^{1–39} due to their acid and redox properties, high thermal stability, simple preparation procedure, and simple physical property modification such as solubility and surface areas^{3,5,7,12–16,18,20,21,26,40,41}. In general, the clusters of HPAs are made up by metal-oxygen anions with different molecular sizes, compositions, and structures^{38,39}. One of the HPAs that has been received much attention is the Keggin-type structure with the formula of $[\text{XM}_{12}\text{O}_{40}]^{n-}$, typically composed of a central XO_4 tetrahedral unit surrounded by twelve octahedrons of MO_6 units, linked by corner- and edge-sharing oxygen atoms. $[\text{PMo}_{12}\text{O}_{40}]^{3-}$ is one of the Keggin-type HPA family, which exhibit two defining characteristics (Bronsted acidity and redox behaviour). $\text{H}_3\text{PMo}_{12}\text{O}_{40}$ (HPMo) and its salts have been reported to show excellent catalytic oxidation of various types of hydrocarbons^{11,14,17,19,23–26,29–32,34,38,39}. The selective oxidation of methacrolein (MAL) to methacrylic acid (MAA) over heteropolyacids has been extensively studied^{1,4,15,26–28,30–32,35–37} since MAA is an important chemical in the production of methyl methacrylate and other derivatives including polymers.

Previous research^{4,29,30,32} has shown that partially substituting Mo with V in the primary Keggin structure enhances the catalytic activity of MAL oxidation to selective form MAA. The vanadyl species in a range of HPA catalysts were investigated for the oxidation and dehydration of methanol²⁵, oxidation of isobutane^{14,24,38} and isobutyric acid^{7,8,11,17}, and partial oxidation of propane²³, for example, ascertaining the role and promotional effect of V on the catalytic activity and product selectivity.

Deußer and co-workers⁴ investigated the effect of V on the kinetics of catalytic MAL oxidation to MAA over various $\text{Cs}_x\text{H}_{3+y-x}\text{PMo}_{12-y}\text{V}_y\text{O}_{40}$ catalysts. It was reported that the presence of V moderately influenced the rate of MAL oxidation but substantially decreased the



rate of MAA oxidation, hence the significant decrease in a consecutive oxidation of MAA and resulting in an increase in the selectivity of MAA.

Song *et al.*¹³ studied the redox properties of several Keggin-type HPA compounds as a function of the counter-cation, heteroatom, and polyatom substitution, in which their reduction potentials were electrochemically measured. They reported that the V-substituted $H_{3+y}PMo_{12-y}V_yO_{40}$ samples demonstrated an increase in the reduction potential in comparison with $H_3PMo_{12}O_{40}$ compound, indicative of different redox properties, which can be tuned and designed for the selective oxidation transformations.

Several studies^{5,16–23,25,26} have been investigated to better understand the nature of the active vanadyl species in the Keggin structure that could promote the selective oxidation reactions. It was reported²² that heteropoly anions, $[PMo_{11}VO_{40}]^{4-}$, in $H_4PMo_{11}VO_{40}$ catalyst were not stable during calcination and reaction, resulting in a partial decomposition and a defect of Keggin structure. This behaviour facilitated the migration of V atom from primary to secondary structures.

Recently, Zhou *et al.*³⁰ reported an in-depth study on vanadyl species for the oxidation of MAL to MAA over three HPA catalysts containing of different vanadyl species in primary and secondary structures, i.e. $H_4PMo_{11}VO_{40}$ (V in the primary structure), $HVO_2PMo_{12}O_{40}$ (V as the form of VO^{2+} in the secondary structure), and $V_2O_5/H_3PMo_{12}O_{40}$ (V as the form of V_2O_5 before calcination under air). It was found that, after calcination of all V-containing HPA catalysts, the vanadyl species were detected as the form of ions, resulting in a breaking of the symmetry of Keggin structure. However, during the oxidation reaction of MAL to MAA, these independent vanadyl ions were transformed into a defective Keggin structure or a squashed square pyramidal form of the Keggin structure. They also reported that $V_2O_5/H_3PMo_{12}O_{40}$ catalyst showed the best catalytic performance due to several active vanadyl species, formed under calcination and reaction conditions. It was concluded that the vanadyl ions, located in the secondary structure, were transformed and interacted with primary Keggin structure during the oxidation of MAL to MAA. Those vanadyl ions were identified as V^{4+} ions, in which its amount was correlated with the selectivity of MAA.

Although the effect and properties of V in HPA catalysts^{4,5,16,26,29,30} in promoting MAL conversion and MAA selectivity have been reported, the mechanistic understanding of the V effect on the surface reaction remains unclear. In particular, the infrared studies on the hydrocarbon-derived surface species under reaction conditions are very limited. In the present work, DRIFTS-MS has been used to gain a better understanding and an insight into the role of



V in the reaction mechanism during the oxidation of MAL to MAA over Keggin-type $\text{H}_3\text{PMo}_{12}\text{O}_{40}$ and $\text{H}_4\text{PMo}_{11}\text{VO}_{40}$ catalysts.

2. Experimental

In this study, both $\text{H}_3\text{PMo}_{12}\text{O}_{40}$ (HPMo) and $\text{H}_4\text{PMo}_{11}\text{VO}_{40}$ (HPMoV) catalysts were obtained from Mitsubishi Chemical Corporation. The catalyst was formed from hydrous 12-molybdophosphoric acid ($\text{H}_3\text{PMo}_{12}\text{O}_{40}\cdot x\text{H}_2\text{O}$, Nippon Inorganic Colour and Chemical Co., Ltd.), extracted from an aqueous solution of $\text{H}_3\text{PMo}_{12}\text{O}_{40}$ and diethyl ether. The $\text{H}_3\text{PMo}_{12}\text{O}_{40}\cdot x\text{H}_2\text{O}$ was then recrystallised from an aqueous solution and the solid dried at 60 °C overnight³⁶.

In situ DRIFTS measurements were performed with a Bruker Tensor 27 FTIR spectrometer equipped with a liquid N_2 -cooled detector. Approximately 40 mg of catalyst sample was placed in a ceramic crucible in the *in situ* DRIFTS cell. The exit lines were connected to a Hiden Analytical HPR20 mass spectrometer in order to monitor the gas phase species: H_2O ($m/z = 18$), MAL ($m/z = 70$), and MAA ($m/z = 86$).

Prior to the DRIFTS experiments, the catalyst was pre-treated by heating in Ar at a total flow rate of $100\text{ cm}^3\text{ min}^{-1}$ ramping the temperature to 320 °C at a rate of 10 C min^{-1} . Once at temperature the catalyst was held for 60 min. Subsequently, the IR spectrum of treated HPA catalyst was taken as a background.

The reactant gases used were MAL (95%, Sigma-Aldrich), O_2 (99.99% BOC), Ar (99.99% BOC). O_2 and Ar were fed from independent Aera™ PC-7700C mass flow controllers. MAL and water vapour were introduced to the system by means of separate saturators with Ar as the carrier gas. The MAL saturator was placed in an ice/water bath and the temperature of H_2O saturator was controlled by Grant™ GD120 thermostatic baths. All the gas lines following the water and MAL saturators were trace heated to prevent condensation. The concentrations of the reactants used were 3500 ppm MAL, 7000 ppm O_2 , 7000 ppm H_2O (when added, and Ar balance. The total flow rate was $100\text{ cm}^3\text{ min}^{-1}$. Gas flows were carefully equilibrated using micrometric needle valves to adjust the pressure between the gas flows on each side of the four-way valve with a high-sensitivity differential pressure detector. This avoided the production of spikes on the MS signal when switching from one mixture to another.



Two different types of *in-situ* DRIFTS-MS experiments were carried out. The first set of experiments was designed to investigate the effect of V on the changes of surface and gas phase species under different gas feeds, i.e. MAL+Ar, MAL+O₂+Ar and MAL+O₂+H₂O+Ar feeds. After Ar pre-treatment, the HPMo catalyst was exposed to each gas feed for 30 min at 320 °C. Our previous work^{36,37} reported the important role of water on the formation of MAA, therefore, the second set of experiments was performed using H₂O switches in and out of the MAL+O₂ feed to probe the role of V. After Ar pre-treatment, the HPMo catalyst was exposed to MAL+O₂ gas feed for only 1 min at 320 °C to allow surface species to be formed and then the cycling switches of H₂O in (5 min) and out (5 min) of the MAL+O₂+Ar feed was performed for 4 cycles.

All *in-situ* DRIFT spectra were recorded with a resolution of 4 cm⁻¹ and with an accumulation of 64 scans every 30 s and the DRIFTS spectra were analysed by OPUS software. The IR data are reported as log 1/R (“absorbance”), with $R = I/I_0$, where R is the sample reflectance, I is the intensity measured under reaction conditions, and I₀ is the intensity measured on the pure HPMo sample under a flow of argon at 320 °C.

3. Results and Discussion

3.1 *In-situ* DRIFTS-MS and IR assignments

3.1.1 Formation of gas phase MAA

Figure 1 shows the comparison of the evolution of gas phase MAA formation under different reaction conditions over HPMo and HPMoV catalyst at 320 °C. Figure 1a shows that, under MAL adsorption conditions, the formation of MAA on HPMoV catalyst rises more rapidly than over HPMo. The formation of gas phase MAA peaks at about 4 and 10 ppm for HPMo and HPMoV, respectively, within 3 min before decreasing slowly to zero over the course of 30 min. This behaviour is due to the depletion of surface oxygen¹². In the presence of O₂, MAA formation does not decrease to zero and there is steady state production as a result of the surface oxygen species being replenished, in agreement with the profile observed without the presence of O₂. Again, HPMoV was found to have a faster production of gaseous MAA than HPMo, reaching the maximum concentration at about 14 ppm in 3 min before gradually decreasing to 10 ppm over 30 min reaction on stream. In comparison, slower MAA formation



was observed over HPMo before reaching the same steady state level at 10 ppm after 10 min under the MAL+O₂ reaction feed. Thereafter, there is no significant difference in MAA formation over the two HPA samples. Similarly, the addition of H₂O into the MAL+O₂ feed (Figure 1c) leads to a further increase in MAA production which is more pronounced over HPMoV than over HPMo. The concentration of MAA on HPMoV reaches *ca.* 22 ppm in 2 min and then slowly decreases to 16 ppm over 30 min reaction time. These results are consistent with previous reports^{36,37}.

View Article Online
DOI: 10.1039/D4CY00552J



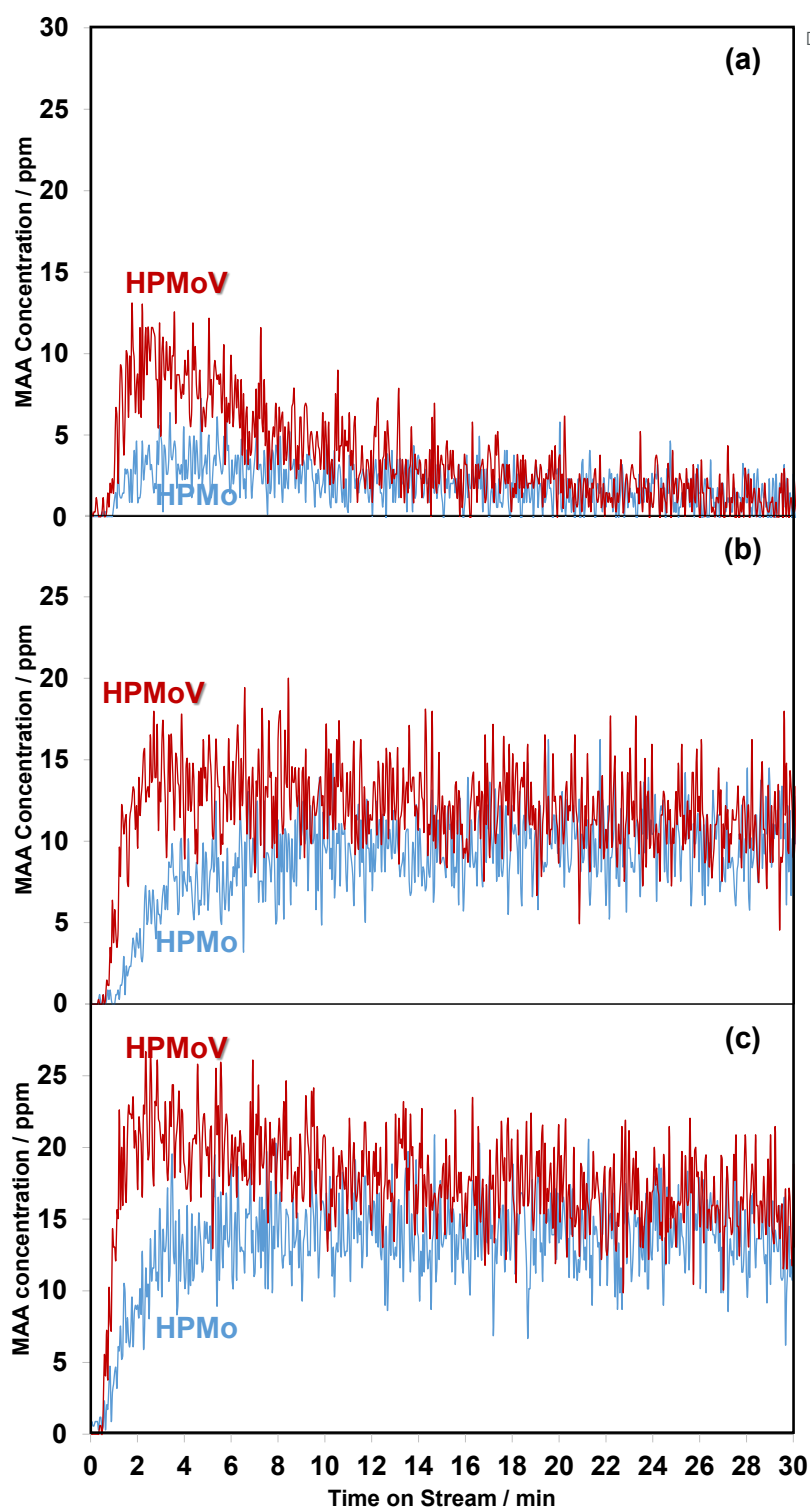


Figure 1 Comparison of the evolution of MAA formation at 320 °C as a function of time on stream over $\text{H}_3\text{PMoO}_{12}\text{O}_{40}$ and $\text{H}_4\text{PMoO}_{11}\text{VO}_{40}$ under MAL (a), MAL+O₂ (b), and MAL+O₂+H₂O (c). Gas feed is composed of 3500 ppm MAL (when added), 7000 ppm O₂ (when added), 7000 ppm H₂O (when added), and Ar balance and the total flow rate is 100 cm³ min⁻¹.



Overall, the current work shows that HPMoV catalyst demonstrates the difference in the release of desirable gas phase MAA product from HPMo catalyst under all three different reaction conditions compared with over HPMoV catalyst at 320 °C. The comparison of *in-situ* DRIFT spectra, recorded at 2 min under different reaction conditions and corresponding to the gaseous MAA profiles displayed in Figure 1, is shown in Figure 2.

3.1.2 *In-situ* DRIFTS and IR assignments

In the current study, the focus of the DRIFTS study has been on the assignment and changes in IR bands appearing in the region of 2100 – 1200 cm^{-1} , associated with hydrocarbon-derived surface species. Figure 2 illustrates the comparison of typical *in situ* DRIFT spectra obtained under MAL, MAL+O₂, and MAL+O₂+H₂O reaction conditions over both HPMo and HPMoV catalysts at 320 °C. Despite the complexity of *in-situ* DRIFT spectra with the rapid accumulation of surface-derived HC species between 2100 and 1200 cm^{-1} , there are three distinct areas for the IR bands at 1800 – 1700 cm^{-1} , 1650 – 1450 cm^{-1} , and below 1400 cm^{-1} . There are typically associated with carbonyl, unsaturated double bonds and carboxylate-type species, and bending vibration of –CH groups, respectively^{9,42–47}. Figure 3 shows a schematic summary of the proposed surface species^{9,36,37,42–47}.

Under MAL adsorption conditions at 320 °C (Figure 2a), KBr was initially used as a inert and reference material. It is clearly observed that the carbonyl (C=O) group of gas-phase MAL at 1715 cm^{-1} is the only significant IR feature, which can also be seen over both HPA catalysts. In contrast to KBr powder, several IR bands were also observed over both HPMo and HPMoV catalysts, Figures S1 and S2, respectively.



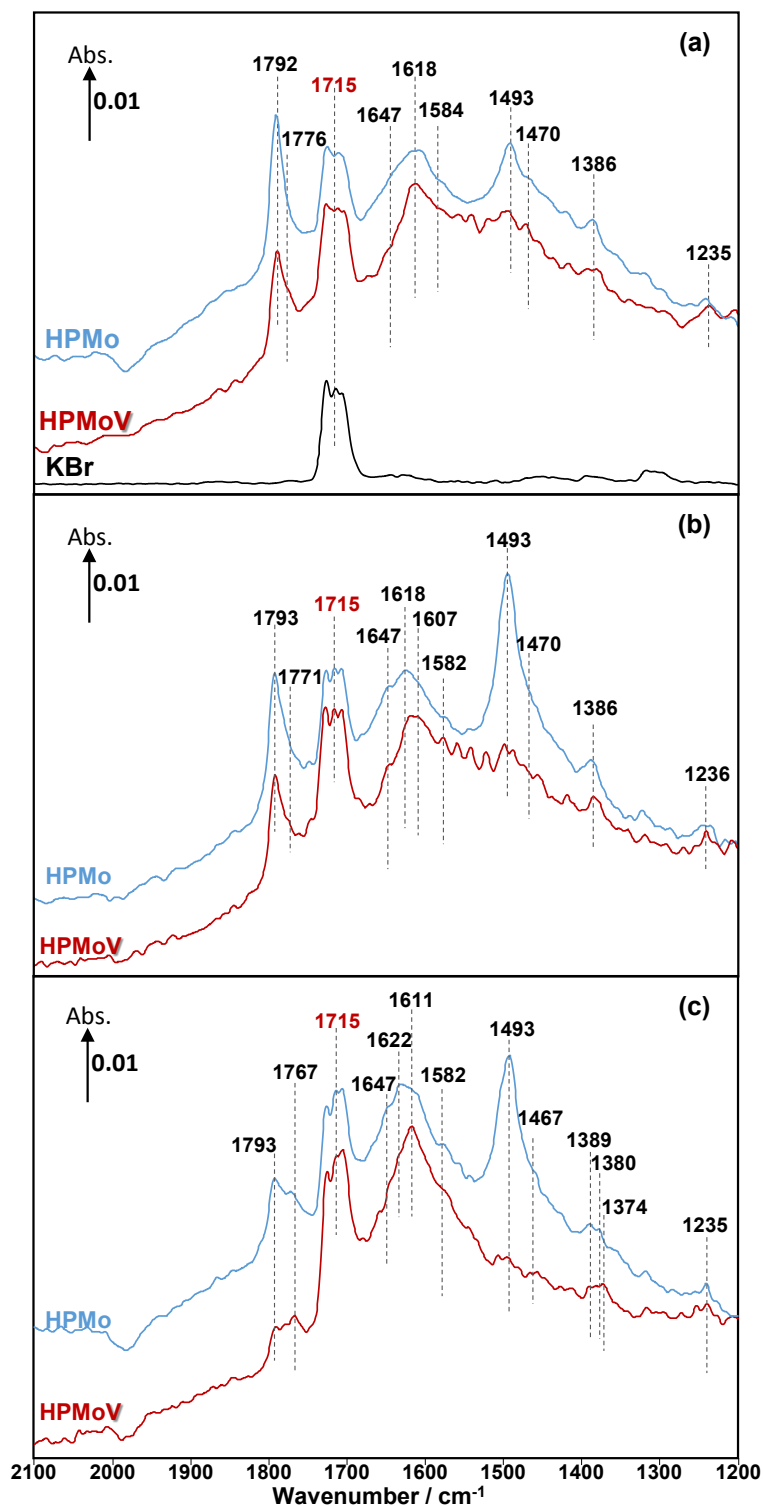


Figure 2 Comparison of *in-situ* DRIFT spectra recorded at 320 °C over $\text{H}_3\text{PMoO}_{12}\text{O}_{40}$ and $\text{H}_4\text{PMoO}_{11}\text{VO}_{40}$ at **2 min** under MAL (a), MAL+O₂ (b), and MAL+O₂+H₂O (c). Gas feed is composed of 3500 ppm MAL (when added), 7000 ppm O₂ (when added), 7000 ppm H₂O (when added), and Ar balance and the total flow rate is 100 cm³ min⁻¹.



Considering the IR bands above 1700 cm^{-1} , in comparison with the gas phase MAI (free $\nu(\text{C}=\text{O})$, 1715 cm^{-1}), the IR band observed at 1793 cm^{-1} would generally be associated with an anhydride species⁴³; however, anhydrides typically consist of two IR bands due to the asymmetric and symmetric stretch of $\text{O}=\text{CO}$. In the present spectra, the additional higher wavenumber IR band/shoulder was not observed, this suggests that the surface species responsible for the band at 1793 cm^{-1} is associated with the formation of cyclic lactone-type adsorbed species, for example **Ads1** and **Ads2** in Figure 3. This feature is at a higher wavenumber than typically found for lactone carbonyl groups ($1750\text{-}1700\text{ cm}^{-1}$) and the shift is likely to be due to the cyclic nature of the lactone formed over the HPA catalysts. However, Schaidle and co-workers⁴⁵ recently carried out the DRIFTS work on the deoxygenation of acetic acid over molybdenum carbides and reported that the double IR bands at $1800\text{--}1780\text{ cm}^{-1}$ are associated with symmetric and asymmetric $\nu(\text{C}=\text{O})$ in monodentate acetates, derived from acetic acid. Our DRIFTS work has shown that the peak at 1793 cm^{-1} appears as a single and strong IR band and is tentatively associated and assigned to $\nu(\text{C}=\text{O})$ group in cyclic lactone.

Figure 2 shows IR bands at 1647 and 1618 cm^{-1} which are attributed to the stretching vibration of unreacted carbon double bonds ($\nu\text{C}=\text{C}$), possibly with different adsorption configurations as bidentate methacrylate adsorbed species (**Ads3**), monodentate methacrylate adsorbed species (**Ads4**), and π -adsorbed species (**Ads5**). The shoulders at 1584 and 1471 cm^{-1} may be associated with the asymmetric and symmetric stretching vibration of carboxylate-type surface species ($\nu_{\text{as}}\text{OCO}$ and $\nu_{\text{s}}\text{OCO}$), respectively. In this case, the formation of bidentate methacrylate adsorbed species (**Ads3**) shifted the vibration of unreacted $\text{C}=\text{C}$ bond to 1647 cm^{-1} due to unconjugated configuration, while the carbonyl group of monodentate methacrylate adsorbed species (**Ads4**) is conjugated with $\text{C}=\text{C}$ bond, resulting in a slightly lower wavenumber of $\text{C}=\text{C}$ bond at 1618 cm^{-1} . It is important to note that the bending vibration of adsorbed and gas phase H_2O , $\delta(\text{HOH})$, is commonly observed in the region of $1670\text{-}1570\text{ cm}^{-1}$ ^{6,37,44}. The presence of this band overlaps with the IR signal of $\text{C}=\text{C}$ bond at 1618 cm^{-1} and its observation becomes increasingly challenging with H_2O accumulation on the catalyst surfaces over the course of the reaction.



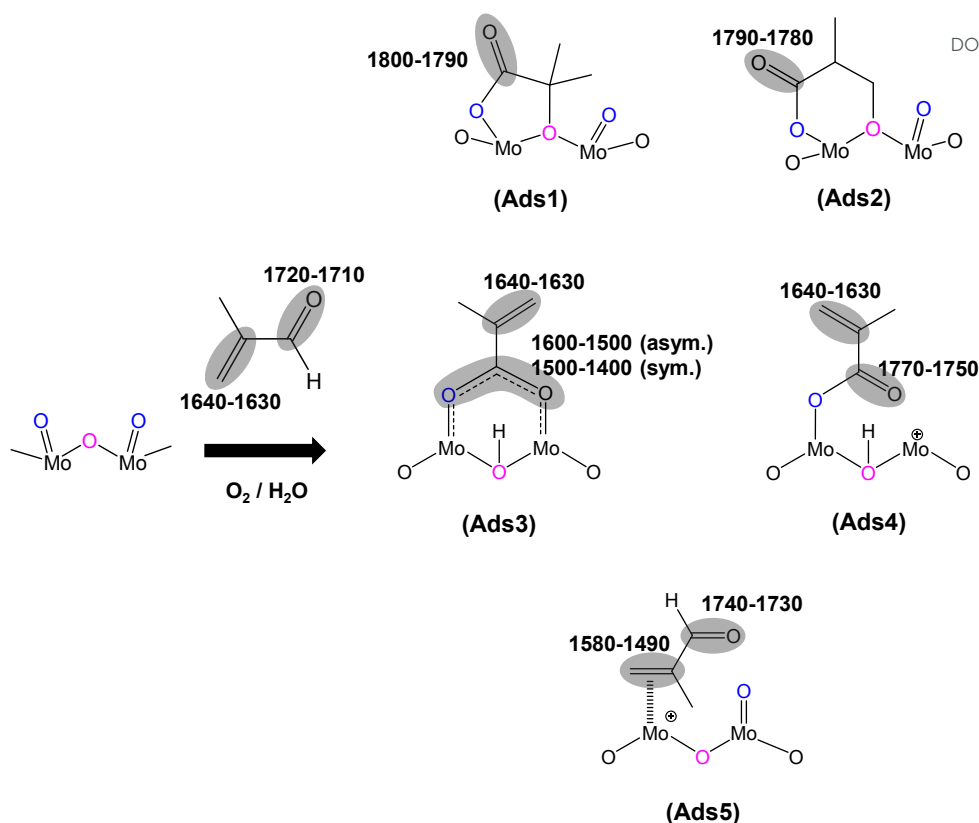


Figure 3 Proposed surface species under MAL reaction conditions at 320 °C over HPA catalysts: 5-membered ring lactone-type species (**Ads1**), 6-membered ring lactone-type species (**Ads2**), bidentate methacrylate species (**Ads3**), monodentate methacrylate species (**Ads4**), and π -adsorbed species [**Ads5**].

Furthermore, a significantly more intense peak at 1493 cm^{-1} was observed over HPMo compared with HPMoV. Krauß *et al.*⁹ carried out the DRIFTS measurements on MAL and MAA adsorptions over $\text{Mo}_9\text{V}_3\text{W}_{12}\text{O}_x$ mixed oxides as well as $\text{C}_8\text{H}_2\text{PMo}_{11}\text{VO}_{40}$ heteropolyacid compound. The IR band observed at 1520 – 1490 cm^{-1} was assigned to π -complex adsorption (**Ads5**) over partially reduced MoO_x . This adsorption can be facilitated by the availability of partially reduced Mo (IV and V) species. However, it is expected that fresh HPA catalysts initially possess the terminal group of $(\text{Mo}=\text{O}_t)$ in the Keggin structure, meaning that π -complex adsorption (**Ads5**) should not be substantially formed over HPA compounds. Therefore, it is likely that the IR band at 1493 cm^{-1} is related to a carboxylate species^{42–46}, for example the bidentate methacrylate adsorbed species (**Ads3**).

In addition to MAL adsorption, the adsorption of MAA on HPMo, HPMoV, and KBr at 320 °C was carried out to help identify the surface species. As shown in Figure 4, on KBr, a



strong carbonyl vibration associated with gas phase MAA was observed which is split into bands at 1768 and 1751 cm^{-1} , due to vibrational stretching of $\nu(\text{C}=\text{O})$ and $\nu(\text{C}-\text{O}^-)$. At 320 $^{\circ}\text{C}$, there is an absence of the $\nu(\text{C}=\text{C})$ stretching band at 1642 cm^{-1} and $\delta(\text{CH}_3)$ bending at 1386 cm^{-1} , which is consistent with the work by Krauß *et al.*⁹. In contrast, over HPMo and HPMoV significant differences in the surface species compared with over KBr were observed when MAA was adsorbed. Strong IR bands at 1795 – 1785 cm^{-1} , assigned to lactone-type adsorbed species (**Ads1** and **Ads2**), were detected with the stretching vibration of unreacted $\nu(\text{C}=\text{C})$ at 1632 cm^{-1} . This is also accompanied by the appearance of the IR bands at 1581, 1491, and 1470 cm^{-1} , which are associated with carboxylate-type surface species^{42–46}. Previously, the adsorption of acetic acid^{42,45,46} also reported that the functional group ($-\text{COOH}$) of acetic acid readily formed the carboxylate species as acetates (H_3CCOO^-) on catalyst surfaces with IR region of 1560 – 1550 cm^{-1} for $\nu_{\text{as}}(\text{COO}^-)$ and with IR region of 1500 – 1450 cm^{-1} for $\nu_{\text{s}}(\text{COO}^-)$ ^{42–46}. Therefore, it is likely that the strong IR band at 1493 – 1491 cm^{-1} is associated with a bidentate methacrylate species (**Ads3**).

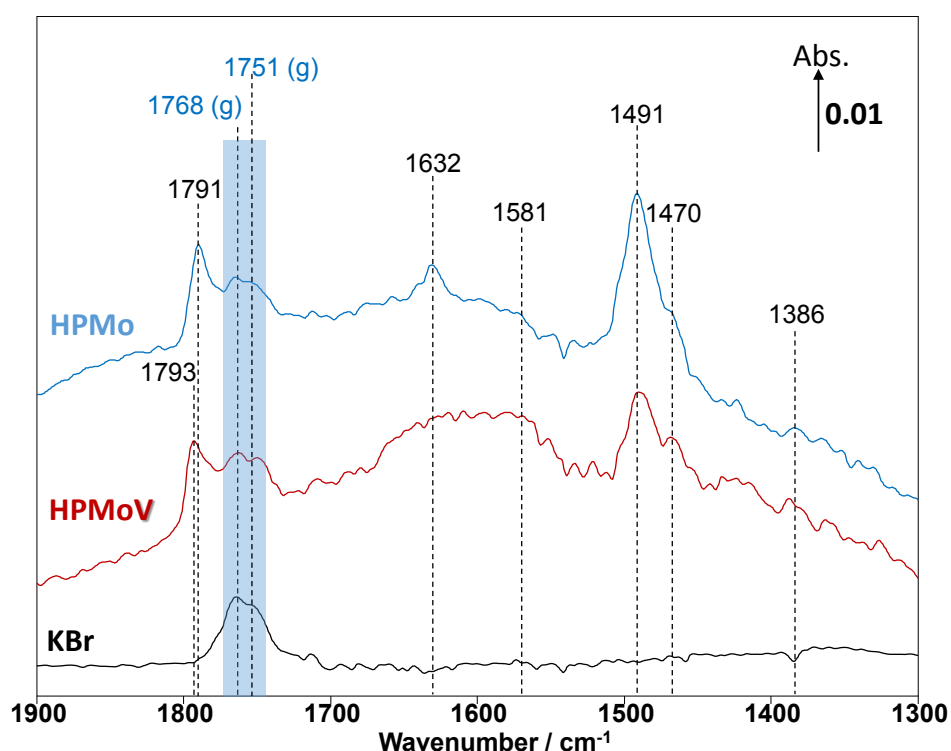


Figure 4 Comparison of *in-situ* DRIFT spectra recorded at **2 min** during the adsorption of methacrylic acid (MAA) at 320 $^{\circ}\text{C}$ over $\text{H}_3\text{PMoO}_{12}\text{O}_{40}$ (HPMo), $\text{H}_4\text{PMoO}_{11}\text{VO}_{40}$ (HPMoV),



and KBr. Gas feed is composed of 3500 ppm MAA and Ar balance and the total flow rate is 100 cm³ min⁻¹. View Article Online
DOI: 10.1039/D4CY00552J

As well as examining MAL adsorption (Figure 2a) at 320 °C over HPAs, MAL+O₂ (Figure 2b) and MAL+O₂+H₂O (Figure 2c) reactions were also carried out under steady state conditions. The similarity in IR features and adsorbed species was observed under all reaction conditions. However, the presence of H₂O in the reaction feed has a direct impact on the formation of monodentate methacrylate adsorbed species (**Ads4**) at around 1767 cm⁻¹, and the occurrence of a lactone-type adsorbed species (**Ads1** and **Ads2**) in the IR of 1795-1785 cm⁻¹. It is important to point out that the IR band at 1793 cm⁻¹ under MAL+O₂+H₂O reaction conditions is less pronounced than those under MAL and MAL+O₂ reaction feeds, i.e. the formation of cyclic lactone-type surface species is hindered or converted by adding H₂O to another adsorbed species. It is also worth noting that both Figures 2 and 4 show similar adsorbed surface species in the IR region of 1770 – 1750 cm⁻¹ under MAA adsorption, MAL adsorption, and MAL+O₂ reaction with and without adding H₂O at 320 °C. Therefore, it is proposed that the observation of the IR bands between 1770 and 1750 cm⁻¹ is associated with the stretching vibration of ν(C=O) group of gas phase MAA or a weakly-bound adsorbed MAA, possibly as monodentate methacrylate surface species (**Ads4**), which can be readily reacted and converted to form gas phase MAA^{27,32,36,37}.

One important feature to be pointed out in both Figures 2 and 4 is that bidentate methacrylate species (**Ads3**) at 1493 – 1491 cm⁻¹ on HPMoV catalyst is less significant than over HPMo. The presence of V in HPMoV catalyst is thought to minimise the formation of bidentate methacrylate species (**Ads3**) but promote the formation of monodentate methacrylate adsorption (**Ads4**). Zhou *et al.*³⁰ proposed that V⁴⁺/VO²⁺ species in the secondary structure rather than primary structure has an influence on the formation and selectivity to MAA during the oxidation reaction of MAL to MAA due to the presence of accessible active vanadyl species. Bayer *et al.*¹⁷ also reported higher catalytic oxidative dehydrogenation of isobutyric acid to MAA on H₄PMo₁₁VO₄₀ than H₃PMo₁₂O₄₀ because H₄PMo₁₁VO₄₀ was reduced and partially decomposed, resulting in more active V⁴⁺ sites during the reaction.

Additional DRIFTS analysis integrating the spectra between 1800 – 1760 cm⁻¹ over the 30 min reaction period has been used to quantify the changes observed. Figures S3 shows the comparison of changes in the ratio of monodentate methacrylate species (**Ads4**) in the IR range of 1770 – 1760 cm⁻¹ to lactone-type adsorbed species (**Ads1** and **Ads2**) between 1800 and 1780



cm⁻¹. It is found that all ratios of monodentate methacrylate species (**Ads4**) to lactone-type surface species (**Ads1** and **Ads2**) under three different reaction conditions at 320 °C over the HPMoV catalyst change more rapidly than those over HPMo catalyst, indicative of faster and more significant formation of monodentate methacrylate surface species (**Ads4**) on the HPMoV catalyst. Therefore, in the present work, it is likely that the reducibility of H₄PMo₁₁VO₄₀ catalyst leads to the formation of these active V⁴⁺/VO²⁺ species³⁰, which facilitates the conversion of bidentate methacrylate species (**Ads3**) to and/or the direct formation of monodentate methacrylate surface species (**Ads4**). As a result, more MAA is formed over HPMoV than HPMo catalysts, as shown in Figure 1.

Recently, Tian *et al.*⁴⁸ reported a density-functional theory (DFT) study and proposed a reaction mechanism which operated via the abstraction of proton from MAL and the formation of monodentate methacrylate species over the bridge oxygen of HPA compounds as a final step to form MAA. The DFT calculations⁴⁸ revealed the formation of monodentate methacrylate species with the lowest reaction energy for HPMoV compound before producing MAA. In addition, the presence of V in HPA compound was found to result in the highest reaction rate constant and lowest activation energy for the change from monodentate methacrylate surface species to gas phase MAA product. Interestingly, the *in-situ* DRIFTS analysis reported, herein, is consistent with this simulation indicating the importance of the formation of monodentate methacrylate adsorbed species (**Ads4**) and the vital role of V present in HPMoV catalyst in enhancing the formation of desirable MAA product.

View Article Online
DOI: 10.1039/C4CY00552J



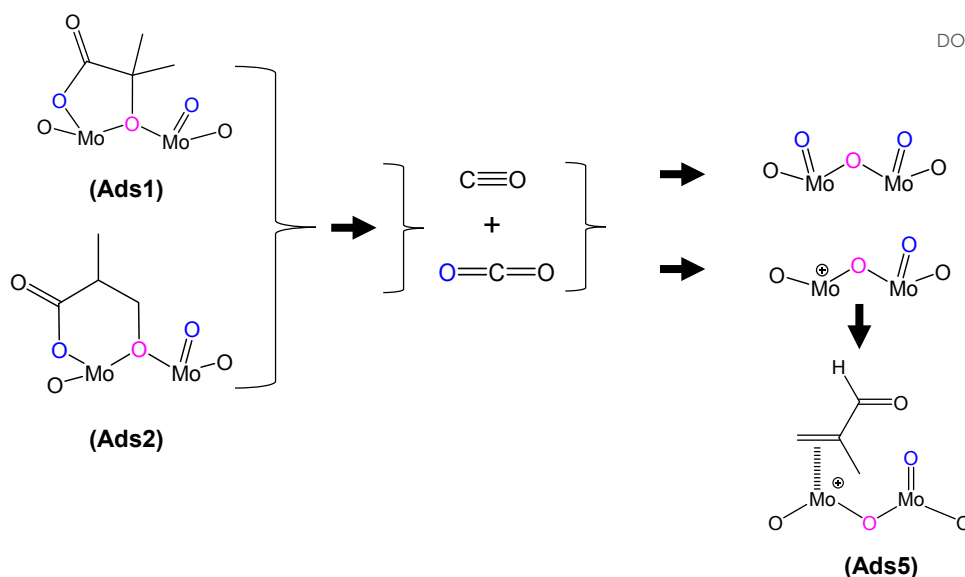


Figure 5 Proposed formation of by-products CO and CO₂, derived from lactone-type adsorbed species during MAL adsorption at 320 °C.

In addition to gaseous MAA formation detected, gas phase CO and CO₂ was also observed as shown in Figures S4 – S6. HPMo was found to produce more CO and CO₂ than HPMoV; however, both catalysts show an initial transient CO and CO₂ formation within 5 min of exposure to the gas feeds. Figure 5 shows the proposed mechanism for the formation of both CO and CO₂ under MAL adsorption (without co-fed O₂) at 320 °C. During MAL adsorption, the HPA surfaces are occupied by bidentate methacrylate adsorbed species (**Ads3**), and that the release of gaseous CO₂ from the surface leads to a partially reduced Mo species, which in turn form the π-adsorbed species (**Ads5**).

In addition to the steady state reaction under different reaction conditions at 320 °C, transient experiments were carried out by performing the switches of H₂O in and out of MAL+O₂ to probe the influence of V on the surface-adsorbed species.

3.2 H₂O Transient Switches

The influence of H₂O on the activity of MAL oxidation and the selectivity of MAA has been reported over HPA^{2,27,28,36,37} and mixed oxides^{49,50} catalysts. Recently, Yasuda *et al.*³⁶ and Chansai *et al.*³⁷ reported the role of water and its involvement in the reaction mechanism over HPMo, where the proton from water is used to form as –OH group in MAA product. Figure 6 shows the changes in gas phase MAA, while Figure 7 demonstrates the evolution of IR bands



in the region of 2100 – 1200 cm^{-1} , corresponding to Figure 6 during the first cycles of H_2O switching in and out of $\text{MAL}+\text{O}_2$ feed at 320 °C.

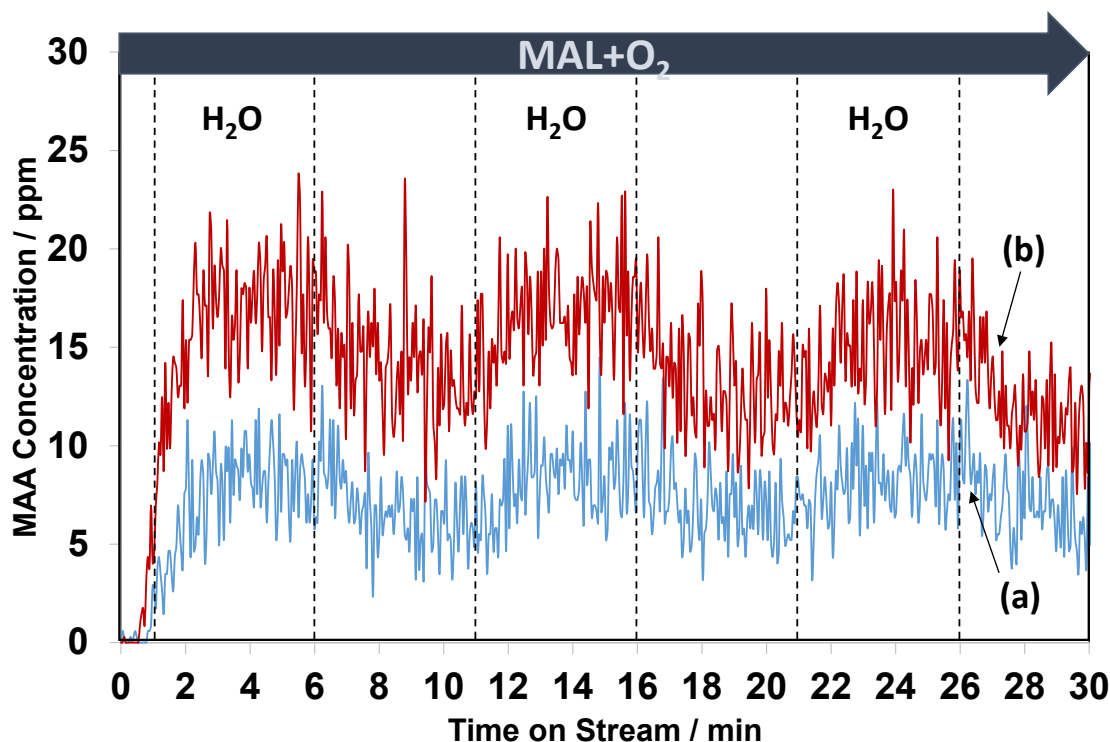


Figure 6 Changes in gaseous MAA product as a function of time on stream at 320 °C over HPMo (a) and HPMoV (b) samples during the switches of H_2O in and out of $\text{MAL}+\text{O}_2$ gas feed. Gas feed is composed of 3500 ppm MAL, 7000 ppm O_2 , 7000 ppm H_2O (when added), and Ar balance and the total flow rate is $100 \text{ cm}^3 \text{ min}^{-1}$.

From Figure 6, regardless of the HPAs used, the production of MAA was promoted by adding H_2O into the $\text{MAL}+\text{O}_2$ gas feed and this is consistent with the previous works^{36,37}. On exposure to $\text{MAL}+\text{O}_2$ reaction conditions for 1 min, MAA was formed at the start of the reaction before adding H_2O . However, an increase in MAA was noticeable over the course of 5 min reaction when H_2O was added. On removing H_2O from the $\text{MAL}+\text{O}_2$ feed, a gradual decrease in concentration of MAA was observed. Further switches of water resulted in similar behaviour with a slow decrease in overall concentration of MAA over the course of 30 min. As noted previously, the formation of MAA over HPMoV catalyst was significantly higher than that over HPMo.



Figure 7 displays the changes in *in-situ* DRIFT spectra corresponding to the changes shown in Figure 6 during the 1st cycle of H₂O switching in and out of MAL+O₂ feed over both HPMo (Figures 7a and 7b) and HPMoV (Figures 7c and 7d) catalysts at 320 °C. Difference *in-situ* DRIFT spectra calculated between the H₂O switches are also provided in Figure S7 for the comparison with Figure 7. In Figure 7a over the HPMo catalyst, a significant formation of lactone-type adsorbed species (**Ads1** and **Ads2**) in the IR range of 1800-1780 cm⁻¹ was initially observed; however, on addition of H₂O to the MAL+O₂ feed, a rapid decrease in these surface species together with the bidentate methacrylate surface species (**Ads3**) at 1493 cm⁻¹ was observed. It was reported^{2,49,51} that the addition of H₂O (-OH group) re-oxidised the reduced MoO₃ surfaces and this may have facilitated the decrease in those adsorbed species as a result of being transformed into more active intermediates, i.e. monodentate methacrylate adsorbed species (**Ads4**). It should also be noted that, although the bidentate methacrylate surface species (**Ads3**) at 1493 cm⁻¹ decreased in the presence of H₂O, these species remained over the HPMo catalyst.

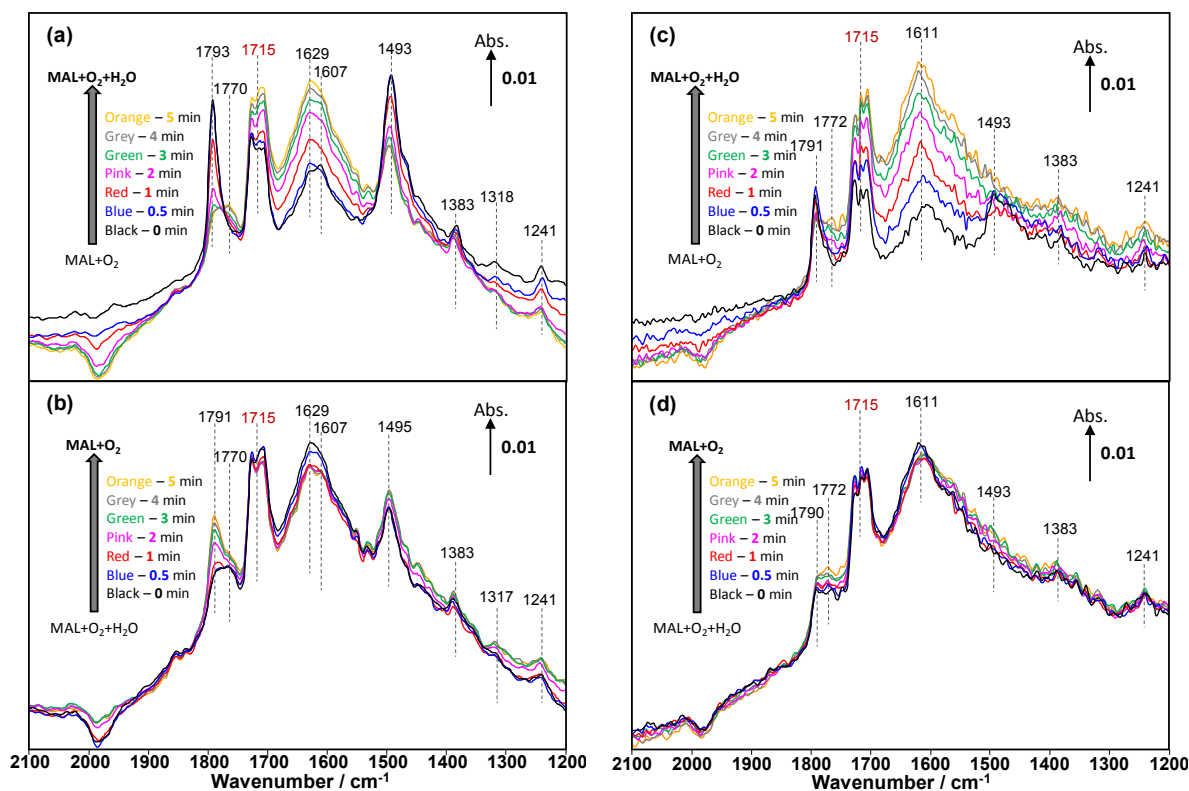


Figure 7 Changes in *in-situ* DRIFT spectra (2100 – 1200 cm⁻¹) corresponding to the formation of MAA shown in Figure 3 as a function of time on stream over HPMo (**a, b**) and HPMoV (**c,d**) catalysts at 320 °C during the 2nd cycle of switches of H₂O in and out of MAL+O₂ gas feed. Gas feed is composed of 3500 ppm MAL, 7000 ppm O₂, 7000 ppm H₂O (when added), and Ar balance and the total flow rate is 100 cm³ min⁻¹.

Chansai *et al.*³⁷ reported *in-situ* DRIFTS-MS analysis in the region of Keggin structure between 1200 and 700 cm⁻¹ during the transient H₂O/D₂O switching experiments on HPMo catalyst at 320 °C and reported the occurrence of H-D exchange, possibly on the bridging oxygen of Mo–O–Mo unit, where H/D atom of water is abstracted. Therein, the H/D recombined with the monodentate carboxylate-type intermediates (proposed as monodentate methacrylate (**Ads4**) in the current work) to produce gas phase MAA. The current DRIFTS analysis shows the formation of monodentate methacrylate species (**Ads4**) is possible and an important intermediate in the final step to form gaseous MAA.

When H₂O was removed from the MAL+O₂ feed in Figure 7b, there is a little change in the monodentate methacrylate species (**Ads4**) at ~1770 cm⁻¹ and bidentate methacrylate adsorbed species (**Ads3**) and/or π -complex (**Ads5**) at 1495 – 1493 cm⁻¹. Only the surface lactone-type species (**Ads1** and **Ads2**) at 1791 cm⁻¹ substantially increased due to the adsorption of MAL under MAL+O₂ reaction conditions. Once H₂O was added again, the oxidation of MAL was enhanced, resulting in an increase of carbonyl of monodentate methacrylate adsorbed species at 1770 cm⁻¹, hence facilitating the formation of gas phase MAA. It is important to point out that the accumulation of surface species under reaction conditions is predominant on the catalyst surfaces and suppresses an observation of evident change in surface species after a couple cycles of experiments.

Similar changes to those surface species over HPMo catalyst were observed for the HPMoV catalyst (Figures 7c and 7d). In the case of the HPMoV catalyst, both adsorbed lactone-type species (**Ads1** and **Ads2**) in the IR range of at 1800-1780 cm⁻¹ and bidentate methacrylate species (**Ads3**) at 1493 cm⁻¹ are smaller than found over HPMo. After H₂O was removed, both adsorbed lactone-type species (**Ads1** and **Ads2**) and monodentate methacrylate species (**Ads4**) increased slightly but the bidentate methacrylate species (**Ads3**) were undetected at 1493 cm⁻¹, probably converted to monodentate methacrylate species (**Ads4**) and/or swamped by the IR signals of H₂O bending vibrations between 1670 and 1400 cm⁻¹.



Figure 6 shows that the formation of gas phase MAA over HPMo is less than that over HPMoV catalyst, it is interesting to note from Figure 7 that both lactone-type adsorbed species (**Ads1** and **Ads2**) at 1793 cm^{-1} and bidentate methacrylate species (**Ads3**) at 1493 cm^{-1} are evidently more pronounced over HPMo than HPMoV catalyst. This suggests that the formation of surface species (**Ads1**, **Ads2**, and **Ads3**) may partially block the active sites for the oxidation reaction of MAL and possibly suppress the formation of MAA to some extent. Conversely, Figure 7 also reveals that monodentate methacrylate adsorbed species (**Ads4**) at 1770 cm^{-1} , which is proposed to be important and associated with MAA product, is more predominant over HPMoV than HPMo catalyst.

To gain an insight into the difference in surface species between the two HPA catalysts, the changes of the two IR ranges of 1800-1780 cm^{-1} , assigned to possibly *unreactive* lactone-type surface spectators (**Ads1** and **Ads2**) and of 1780-1760 cm^{-1} , assigned to possibly *active* monodentate methacrylate intermediates (**Ads4**) were compared. Figure 8 shows the comparison of the evolution of the ratio of monodentate methacrylate adsorbed species (**Ads4**) to lactone-type adsorbed species (**Ads1** and **Ads2**) during H_2O switches in and out of MAL+ O_2 feed at 320 $^\circ\text{C}$. It has been found that the difference in the profile of those surface species between HPMo and HPMoV catalysts is somewhat interesting. It is clearly seen that HPMoV catalyst demonstrates the continuous rise while HPMo catalyst shows both increase and decrease in the ratio of those species with respect to the switches of H_2O in and out of MAL+ O_2 feed over the course of 30 min.

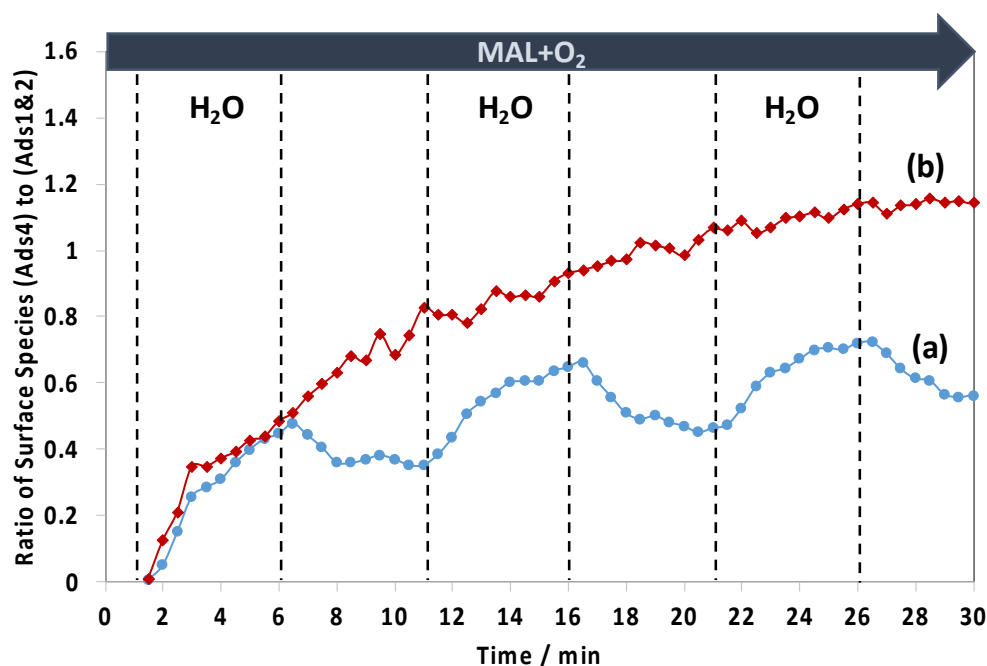


Figure 8 Changes in the ratio of monodentate methacrylate adsorbed species (**Ads4**) in the IR range of 1780 – 1760 cm⁻¹ to lactone-type adsorbed species (**Ads1** and **Ads2**) in the IR range of 1800 – 1780 cm⁻¹ as a function of time on stream at 320 °C over HPMo (a) and HPMoV (b) catalysts during the switches of H₂O in and out of MAL+O₂ feed. Gas feed is composed of 3500 ppm MAL, 7000 ppm O₂, 7000 ppm H₂O (when added), and Ar balance and the total flow rate is 100 cm³ min⁻¹.

Examining Figure 8 between 1 and 6 min when H₂O is first introduced to the MAL+O₂ gas feed, it is found that the ratio of monodentate methacrylate adsorbed species (**Ads4**) to lactone-type adsorbed species (**Ads1** and **Ads2**) for HPMoV shows an initial rise which is slightly faster than found for HPMo. This means that the formation of monodentate methacrylate adsorbed species (**Ads4**) is more pronounced than lactone-type adsorbed species (**Ads1** and **Ads2**). This suggests the faster formation of monodentate methacrylate surface species (**Ads4**), the more rapid formation of gaseous MAA product as seen in Figure 5 where gaseous MAA is produced more significantly over HPMoV than HPMo catalyst. Interestingly, our DRIFTS-MS analysis strongly suggests that the formation of monodentate methacrylate adsorbed species (**Ads4**) is potentially important intermediates and has a significant role in facilitating the formation of gas phase MAA product.

In contrast, in the absence of H₂O between 6 and 11 min, the ratio of monodentate methacrylate adsorbed species (**Ads4**) to lactone-type adsorbed species (**Ads1** and **Ads2**) on HPMo catalyst was decreased, indicative of a more significant increase of lactone-type adsorbed species (**Ads1** and **Ads2**) than monodentate methacrylate adsorbed species (**Ads4**). It is worth noting that a different trend was observed over the HPMoV catalyst, in which the ratio of monodentate methacrylate adsorbed species (**Ads4**) to lactone-type adsorbed species (**Ads1** and **Ads2**) continues to rise, indicating that monodentate methacrylate adsorbed species (**Ads4**) is more pronounced than lactone-type adsorbed species (**Ads1** and **Ads2**). The difference in these ratios between HPMo and HPMoV catalysts suggests that the presence of V in the Keggin structure of HPA has a direct influence on the formation of monodentate methacrylate surface species (**Ads4**) rather than that of lactone-type adsorbed species (**Ads1** and **Ads2**) under reaction conditions at 320 °C.

Interestingly, there is the difference in how the surface monodentate methacrylate species (**Ads4**) change over HPMo and HPMoV catalysts, as shown in Figure 8. The continuous rise of the ratio of monodentate methacrylate adsorbed species (**Ads4**) to lactone-



type adsorbed species (**Ads1** and **Ads2**) for HPMoV catalyst during H₂O switches in and out of MAL+O₂ reaction over HPMoV is proposed to be due to differences in the amount of V⁴⁺ species present. The V 2p_{3/2} XPS spectra (Figure S8) shows two vanadyl species present in the Keggin structure, i.e. V⁵⁺ at 517.7 eV and V⁴⁺ at 516.5 eV^{29,30,35}, and there is a difference in the ratio of V⁴⁺ to V⁵⁺ species between both fresh and spent HPMoV catalyst, which is 0.29 and 0.82, respectively. This increase in the ratio of V⁴⁺ to V⁵⁺ species between the fresh and spent HPMoV sample after 60 min under MAL+O₂+H₂O reaction conditions at 320 °C is consistent with the proposal that the amount of V⁴⁺ in HPMoV catalyst could be responsible for the formation of methacrylic acid (MAA) and the formation of monodentate methacrylate species (**Ads4**) under reaction conditions with and without H₂O. Zhou *et al.*³⁰ also reported that the amount of V⁴⁺ is correlated with methacrylic acid formation. This change in oxidation state of vanadyl species from V⁵⁺ to V⁴⁺ species may also explain the continuous rise of the ratio of monodentate methacrylate adsorbed species (**Ads4**) to lactone-type adsorbed species (**Ads1** and **Ads2**) for HPMoV catalyst due to (1) an increase in V⁴⁺/VO²⁺ species as proposed by Zhou *et al.*³⁰ and (2) the high reaction rate constant and low activation energy to form the monodentate methacrylate species as recently reported by Tian and co-workers⁴⁸.

Additionally, we have investigated the acid property of both HPMo and HPMoV catalysts using *in-situ* DRIFTS technique and pyridine adsorption at 320 °C. The comparison of *in-situ* DRIFT spectra of pyridine adsorption at 320 °C (recorded at 10 min under Ar purge after the pyridine adsorption at 30 °C for 60 min) for both HPMo and HPMoV catalysts is shown in Figure S9. Interestingly, the ratio of Brønsted to Lewis acid sites on HPMoV (57.7) is much greater than that on HPMo (14.9). Consistent with this study, previous studies⁵²⁻⁵⁶ were carried out to investigate the acid property of HPA compounds and showed that strong Brønsted acid sites facilitated the activation of MAL due to an increase in the electrophilicity of carbonyl carbon of MAL.⁵⁵ This led to an enhancement of catalytic oxidation activity and the formation of desirable MAA product via the repulsive interaction between Brønsted sites and acidic MAA product. These Brønsted acid sites perhaps explains the observation of the present work that HPMoV catalyst exhibits faster and more formation of active monodentate methacrylate adsorbed species (**Ads4**) to produce gas phase MAA than HPMo catalyst as presented in Figures 6, 7 and 8.

It is important to note that the continuous rise of the ratio of monodentate methacrylate adsorbed species (**Ads4**) to lactone-type adsorbed species (**Ads1** and **Ads2**) for HPMoV



catalyst indicates that the surfaces of HPMoV can also act as the reservoir of monodentate methacrylate adsorbed species (**Ads4**). This is likely due to (1) a greater number of V^{4+}/VO^{2+} active sites as reported by Zhou and co-workers³⁰ that the substitution of Mo with V in the Keggin structure can possess the abundance of V^{4+}/VO^{2+} active sites, which influenced the redox property for better redox active sites through faster reduction and re-oxidation steps and somewhat had a direct relation to the catalytic activity and the selectivity of MAA and (2) Brønsted acid sites present in HPMoV catalyst, where both *inactive* and *active* surface species with the same chemical composition and structure detected by *in-situ* DRIFTS are more rapidly formed than HPMo catalyst. Only a small portion of monodentate methacrylate adsorbed species (**Ads4**) converted or reacted to produce MAA on HPMoV catalyst.

4. Conclusions

The current work reports, for the first time, the *in-situ* DRIFTS-MS analysis to gain an insight into the role and effect of V on the formation of MAA during the selective oxidation of MAL to MAA over HPA catalysts. Under different reaction conditions at 320 °C, the MS results show that the presence of V in HPMoV catalyst yields higher formation of gas phase MAA product than HPMo catalyst. Simultaneously, the *in-situ* DRIFTS analysis reveals that several possible HC-adsorbed species have been formed and tentatively identified: 5-membered ring of lactone-type adsorbed species (**Ads1**), 6-membered ring of lactone-type adsorbed species (**Ads2**), bidentate methacrylate adsorbed species (**Ads3**), monodentate methacrylate adsorbed species (**Ads4**), and π -adsorbed MAL species (**Ads5**). Interestingly, the transient switching of H₂O in and out of MAL+O₂ gas feed reveals that the substitution of Mo with V in the Keggin primary structure selectively and substantially facilitates the formation of monodentate methacrylate adsorbed species (**Ads4**) in the final step before forming gas phase MAA. It is important to point out that the current work reports the influence of V in HPMoV catalyst on the surface adsorbed species under various reaction conditions in comparison with HPMo compound. However, the reaction mechanism of MAL to MAA between the two catalysts is not differentiated. It is likely that the same mechanism of selective oxidation of MAL occurs but only the presence of V in the Keggin primary structure of HPMoV catalyst facilitates more formation of reactive monodentate methacrylate intermediates (**Ads4**), resulting in further enhancement of gaseous MAA formation when comparing with HPMo catalyst.



Conflicts of Interest

There are no conflicts to declare.

Acknowledgements

We gratefully acknowledge the financial support of this work from Mitsubishi Chemical Corporation.

References

- 1 Y. Konishi, K. Sakata, M. Misono and Y. Yoneda, *Journal of Catalysis*, 1982, **77**, 169–179.
- 2 V. Ernst, Y. Barboux and P. Courtine, *Catalysis Today*, 1987, **1**, 167–180.
- 3 K. Eguchi, T. Seiyama, N. Yamazoe, S. Katsuki and H. Taketa, *Journal of Catalysis*, 1988, **111**, 336–344.
- 4 L. M. Deußer, J. W. Gaube, F.-G. Martin and H. Hibst, in *11th International Congress On Catalysis - 40th Anniversary*, eds. J. W. Hightower, W. Nicholas Delgass, E. Iglesia and A. T. B. T.-S. in S. S. and C. Bell, Elsevier, 1996, vol. 101, pp. 981–990.
- 5 K. Inumaru, A. Ono, H. Kubo and M. Misono, *Journal of the Chemical Society, Faraday Transactions*, 1998, **94**, 1765–1770.
- 6 A. M. Herring and R. L. McCormick, *The Journal of Physical Chemistry B*, 1998, **102**, 3175–3184.
- 7 C. Marchal-Roch, N. Laronze, N. Guillou, A. Tézé and G. Hervé, *Applied Catalysis A: General*, 2000, **199**, 33–44.
- 8 C. Marchal-Roch, N. Laronze, N. Guillou, A. Tézé and G. Hervé, *Applied Catalysis A: General*, 2000, **203**, 143–150.
- 9 K. Krauß, A. Drochner, M. Fehlings, J. Kunert and H. Vogel, *Journal of Molecular Catalysis A: Chemical*, 2000, **162**, 413–422.
- 10 S. Ganapathy, M. Fournier, J. F. Paul, L. Delevoye, M. Guelton and J. P. Amoureux, *Journal of the American Chemical Society*, 2002, **124**, 7821–7828.
- 11 C. Marchal-Roch, N. Laronze, R. Villanneau, N. Guillou, A. Tézé and G. Hervé, *Journal of Catalysis*, 2000, **190**, 173–181.
- 12 M. Misono, *Chemical Communications*, 2001, 1141–1152.
- 13 I. K. Song and M. A. Barteau, *Journal of Molecular Catalysis A: Chemical*, 2004, **212**, 229–236.
- 14 N. Ballarini, F. Candiracci, F. Cavani, H. Degrand, J.-L. Dubois, G. Lucarelli, M. Margotti, A. Patinet, A. Pigamo and F. Trifirò, *Applied Catalysis A: General*, 2007, **325**, 263–269.
- 15 H. Kim, J. C. Jung, S. H. Yeom, K.-Y. Lee and I. K. Song, *Journal of Molecular Catalysis A: Chemical*, 2006, **248**, 21–25.
- 16 H. Kim, J. C. Jung, D. R. Park, S.-H. Baeck and I. K. Song, *Applied Catalysis A: General*, 2007, **320**, 159–165.
- 17 R. Bayer, C. Marchal-Roch, F. X. Liu, A. Tézé and G. Hervé, *Journal of Molecular Catalysis A: Chemical*, 1996, **114**, 277–286.



- 18 V. F. Odyakov, E. G. Zhizhina and K. I. Matveev, *Journal of Molecular Catalysis A: Chemical*, 2000, **158**, 453–456. [View Article Online](#)
DOI: 10.1039/D4CY00552J
- 19 P. Villabrilie, G. Romanelli, P. Vázquez and C. Cáceres, *Applied Catalysis A: General*, 2004, **270**, 101–111.
- 20 G. Mestl, T. Ilkenhans, D. Spielbauer, M. Dieterle, O. Timpe, J. Kröhnert, F. Jentoft, H. Knözinger and R. Schlögl, *Applied Catalysis A: General*, 2001, **210**, 13–34.
- 21 C. Marchal-Roch, C. Julien, J. F. Moisan, N. Leclerc-Laronze, F. X. Liu and G. Hervé, *Applied Catalysis A: General*, 2004, **278**, 123–131.
- 22 T. Ressler, O. Timpe, F. Girgsdies, J. Wienold and T. Neisius, *Journal of Catalysis*, 2005, **231**, 279–291.
- 23 X.-K. Li, J. Zhao, W.-J. Ji, Z.-B. Zhang, Y. Chen, C.-T. Au, S. Han and H. Hibst, *Journal of Catalysis*, 2006, **237**, 58–66.
- 24 A. Brückner, G. Scholz, D. Heidemann, M. Schneider, D. Herein, U. Bentrup and M. Kant, *Journal of Catalysis*, 2007, **245**, 369–380.
- 25 J. E. Molinari, L. Nakka, T. Kim and I. E. Wachs, *ACS Catalysis*, 2011, **1**, 1536–1548.
- 26 Y.-L. Cao, L. Wang, L.-L. Zhou, G.-J. Zhang, B.-H. Xu and S.-J. Zhang, *Industrial & Engineering Chemistry Research*, 2017, **56**, 653–664.
- 27 M. Kanno, T. Yasukawa, W. Ninomiya, K. Ooyachi and Y. Kamiya, *Journal of Catalysis*, 2010, **273**, 1–8.
- 28 M. Kanno, Y. Miura, T. Yasukawa, T. Hasegawa, W. Ninomiya, K. Ooyachi, H. Imai, T. Tatsumi and Y. Kamiya, *Catalysis Communications*, 2011, **13**, 59–62.
- 29 F. Jing, B. Katryniok, F. Dumeignil, E. Bordes-Richard and S. Paul, *Journal of Catalysis*, 2014, **309**, 121–135.
- 30 L. Zhou, L. Wang, S. Zhang, R. Yan and Y. Diao, *Journal of Catalysis*, 2015, **329**, 431–440.
- 31 L. Zhou, L. Wang, Y. Cao, Y. Diao, R. Yan and S. Zhang, *Molecular Catalysis*, 2017, **438**, 47–54.
- 32 Y.-L. L. Cao, L. Wang, B.-H. H. Xu and S.-J. J. Zhang, *Chemical Engineering Journal*, 2018, **334**, 1657–1667.
- 33 Y. Geng, S. Xiong, B. Li, Y. Liao, X. Xiao and S. Yang, *Industrial & Engineering Chemistry Research*, 2018, **57**, 856–866.
- 34 X. Li, J. Zhang, F. Zhou, Y. Wang, X. Yuan and H. Wang, *Molecular Catalysis*, 2018, **452**, 93–99.
- 35 L. Zhou, S. Zhang, Z. Li, J. Scott, Z. Zhang, R. Liu and J. Yun, *RSC Adv.*, 2019, **9**, 34065–34075.
- 36 S. Yasuda, J. Hirata, M. Kanno, W. Ninomiya, R. Otomo and Y. Kamiya, *Applied Catalysis A: General*, 2019, **570**, 164–172.
- 37 S. Chansai, Y. Kato, W. Ninomiya and C. Hardacre, *Faraday Discussions*, 2021, **229**, 443–457.
- 38 L. Zhang, S. Paul, F. Dumeignil and B. Katryniok, *Catalysts*, 2021, **11**, 769.
- 39 M. J. da Silva, A. A. Rodrigues and N. P. G. Lopes, *Inorganics*, 2023, **11**, 162.
- 40 M. Misono, K. Sakata, Y. Yoneda and W. Y. Lee, in *Studies in Surface Science and Catalysis*, eds. T. Seiyama and K. Tanabe, Elsevier, 1981, vol. 7, pp. 1047–1059.
- 41 N. Essayem, G. Coudurier, M. Fournier and J. C. Védrine, *Catalysis Letters*, 1995, **34**, 223–235.
- 42 W. Rachmady and M. A. Vannice, *Journal of Catalysis*, 2002, **208**, 170–179.
- 43 S. Kohl, A. Drochner and H. Vogel, *Catalysis Today*, 2010, **150**, 67–70.
- 44 G. Ya. Popova, Y. A. Chesalov, E. M. Sadovskaya and T. V. Andrushkevich, *Journal of Molecular Catalysis A: Chemical*, 2012, **357**, 148–153.



- 45 J. A. Schaidle, J. Blackburn, C. A. Farberow, C. Nash, K. X. Steirer, J. Clark, D. J. Robichaud and D. A. Ruddy, *ACS Catal.*, 2016, **6**, 1181–1197. View Article Online
DOI:10.1039/D4CY00552J
- 46 M. Zhou, H. Zhang, H. Ma and W. Ying, *Fuel Processing Technology*, 2016, **144**, 115–123.
- 47 H. Alalwan and A. Alminshid, *Spectrochimica Acta Part A: Molecular and Biomolecular Spectroscopy*, 2020, **229**, 117990.
- 48 Y. Tian, H. Yan, J. Li, Y. Yang, T. Guo, X. Zhang, S. Xiang and C. Li, *Ind. Eng. Chem. Res.*, 2024, **63**, 4807–4816.
- 49 H. Böhnke, J. Gaube and J. Petzoldt, *Industrial & Engineering Chemistry Research*, 2006, **45**, 8794–8800.
- 50 H. Böhnke, J. Gaube and J. Petzoldt, *Industrial & Engineering Chemistry Research*, 2006, **45**, 8801–8806.
- 51 S. Kwon, P. Deshlahra and E. Iglesia, *Journal of Catalysis*, 2018, **364**, 228–247.
- 52 I. K. Song, M. S. Kaba and M. A. Barteau, *J. Phys. Chem.*, 1996, **100**, 17528–17534.
- 53 M. J. Janik, R. J. Davis and M. Neurock, *Catalysis Today*, 2005, **105**, 134–143.
- 54 A. M. Alsalme, P. V. Wiper, Y. Z. Khimyak, E. F. Kozhevnikova and I. V. Kozhevnikov, *Journal of Catalysis*, 2010, **276**, 181–189.
- 55 S. Yasuda, A. Iwakura, J. Hirata, M. Kanno, W. Ninomiya, R. Otomo and Y. Kamiya, *Catalysis Communications*, 2019, **125**, 43–47.
- 56 C. Pezzotta, V. S. Marakatti and E. M. Gaigneaux, *Catal. Sci. Technol.*, 2020, **10**, 7984–7997.



Data Availability Statements

View Article Online
DOI: 10.1039/D4CY00552J

The data supporting this article have been included as part of the Supplementary Information.

